Structural characterization of an α-1, 6-linked galactomannan from natural *Cordyceps*

sinensis

Junqiao Wang [a], Shaoping Nie [a], Shuping Chen [a], Aled O. Phillips [b], Glyn O. Phillips [c], Yajing Li [d], Mingyong Xie [a*], Steve W. Cui [a,e]

[a] State Key Laboratory of Food Science and Technology, Nanchang University, 235 Nanjing East Road, Nanchang, Jiangxi Province, 330047, China

[b] School of Medicine, University of Cardiff, Wales, UK

[c] Phillips Hydrocolloids Research Centre, Glyndwr University, Wrexham, LL11 2AW Wales, UK

[d] Qinghai Ta Er Sheng Gu Agricultural Science and Technology Co. Ltd., Xining 810003, China

[e] Guelph Research and Development Centre, Agriculture and Agri-Food Canada, 93 Stone Road West, Guelph, Ontario, N1G 5C9, Canada

* Corresponding authors:

myxie@ncu.edu.cn (Professor Mingyong Xie, PhD), Tel. & Fax: +86-791-83969009.

Steve.Cui@agr.gc.ca (Professor Steve W. Cui, PhD),Tel.: +1-5197808028; Fax: +1-5198292600.

Abstract

An α-1, 6-linked galactomannan was isolated and purified from natural *Cordyceps sinensis*. The fine structure analysis of this polysaccharide was elucidated based on partial acid hydrolysis, monosaccharide composition, methylation and 1D/2D nuclear magnetic resonance (NMR) spectroscopy. Monosaccharide composition analysis revealed that this polysaccharide was mainly composed of galactose (68.65%), glucose (6.65%) and mannose (24.02%). However, after partial acid hydrolysis the percentages of galactose, glucose and mannose were changed to 3.96%, 13.82% and 82.22%, respectively. The molecular weight of this polysaccharide was 7207. Methylation and NMR analysis revealed that this galactomannan had a highly branched structure, mainly consisted of a mannan skeleton and galactofuranosyl chains. The structure of galactofuranosyl part was formed by alternating (1→5)-lined β-Gal*f* and (1→6)-liked β-Gal*f* or a single (1→6)-liked β-Gal*f*, attaching to the *O*-2 and *O*-4 of the mannose chain, and terminated at β-T-Gal*f*. The mannan core was revealed by analyzing the partial acid hydrolysate of the galactomannan and the structure was composed of (1→6)-linked α-Man*p* backbone, with substituted at C-2 by short chains of 2-substituted Man*p* or Gal*f* branches.

Key words: natural *Cordyceps sinensis*; low molecular weight polysaccharide; alkali extraction; structure

1. Introduction

Cordyceps sinensis (Berk.) Sacc., called "DongChongXiaCao" in Chinese, is a valued Chinese caterpillar fungus that has been extensively used as tonic and medicinal food for more than 700 years. It was mainly distributed in the prairie soil at altitudes of above 3500 meters in the Qinghai-Tibetan Plateau. *C. sinensis* has a wide-range of nutritional and pharmacological benefits on the immune, circulatory, cardiovascular, hematogenic and respiratory systems (Chen, Wang, Nie, & Marcone, 2013). These beneficial effects might be attributed to a number of bioactive compounds that has been detected in *C. sinensis*, including polysaccharide, amino acids, fatty acids, minerals, mannitol and nucleoside (Wang, et al., 2015). Among them, the polysaccharide had been widely studied for their potent activities such as anti-tumor, antioxidant, immunomodulatory, hypoglycemic, *etc.* (Nie, Cui, Xie, Phillips, & Phillips, 2013).

The polysaccharide is mainly presented in the walls of the fungal cells. It was reported that the fungal cell wall is composed of two major kinds of polysaccharides, a rigid fibrillary of chitin (or cellulose) and a matrix-like glucan or glycoproteins (Zhang, Cui, Cheung, & Wang, 2007). Besides, a small proportion of water-soluble galactomannan was also found in the surface of fungal wall using dilute alkali extraction (Leal, Prieto, Bernabé, & Hawksworth, 2010). In most cases, the chemical structure of these galactomannans was similar, with a mannan backbone and branching galactosyl residues as the common units. In our previous study, we have characterized the structure of a bioactive hydrophilic glucan (CBHP) from *C. sinensis*, which was comprised a main chain of α-1,4- Glc*p* and α-1,3-Glc*p*, and a side chain of α-T-Glc*p*, with branching point at O-2 or O-6 (Nie, et al., 2011). To date, the galactomannan structure has been also revealed in *C. sinensis*, but not very commonly reported. In early 1977, Miyazaki *et al.* reported a purified galactomannan, CS-I, from ascocarps of *C. sinensis*, consisting of mannan chain with α-1,2- Man*p* residues and galactosyl oligomer containing branches (Miyazaki, Oikawa, & Yamada, 1977). Using 5% sodium carbonate extraction, Kiho *et al.* obtained a water-soluble, minor protein-containing galactomannan (CT-4N), which mainly consisted of α-1,6- Man*p* and α-1,2- Man*p* in the main chain and a large proportion of β-1,5-Gal*f* in the branches (Kiho, Tabata, Ukai, & Hara, 1986). However, the detailed structure of these galactomannans has not yet been achieved.

Therefore, in order to obtain a comprehensive knowledge of the polysaccharides from *C. sinensis*,

75 we successfully separated a highly purified galactomannan from the water-insoluble residues of

76 natural *C. sinensis* and further characterized the chemical structure of this polysaccharide by

77 molecular weight, monosaccharide composition, methylation, partial acid hydrolysis and 1D/2D

78 NMR spectroscopy.

79 **2.   Materials and Methods**

80 2.1.   Materials

81 The dried natural *C. sinensis* was collected from Qinghai province, China. Monosaccharide

82 standards, including fucose (Fuc), rhamnose (Rha), arabinose (Ara), galactose (Gal), glucose (Glc),

83 mannose (Man), xylose (Xyl), fructose (Fru), ribose (Rib), galacturonic acid (GalA) and glucuronic

84 acid (GlcA) were purchased from Sigma-Aldrich (St. Louis, MO, USA). Deuterium oxide (D_2O)

85 and sodium borodeuteride ($NaBD_4$, 98 atom % D) were from Acros Organics (New Jersey, USA).

86 All the other reagents were of analytical grade unless specified.

87 2.2.   Isolation and purification of the polysaccharide

88 The flowchart for the extraction and fractionation procedure was shown in **Fig. 1a**. Briefly, the

89 powder of natural *C. sinensis* after exhaustively extracting with hot water was collected and dried.

90 It was then extracted with 0.5 $mol \cdot L^{-1}$ NaOH/0.01 $mol \cdot L^{-1}$ $NaBH_4$ at 4 ºC two times, each for 12 h.

91 After centrifugation, all the supernatant was collected and neutralized with 1 $mol \cdot L^{-1}$ HAc. The

92 solution was then centrifuged again to separate the supernatant, achieving the alkali extraction

93 water-soluble fraction. After dialysis and precipitation with ethanol, a crude polysaccharide was

94 obtained. Subsequently, the protein was removed by Sevag method (chloroform/1-butanol, v/v =

95 4:1) and protease (Megazyme, Ireland) hydrolysis, and then dialysis and further froze dry to get the

96 alkali-extractable polysaccharide from natural *C. sinensis*. The alkali-extractable polysaccharide

97 was then fractionated and purified by precipitating with ethanol repeatedly, and the supernatant, the

98 major fraction, was collected for the following analysis.

99 2.3.   Partial acid hydrolysis

100 The polysaccharide (~45 mg) was hydrolyzed with 0.1 $mol \cdot L^{-1}$ TFA (10 mL) at 100 ºC for 0.5 h, 1

101 h and 2 h, respectively. After cooling to room temperature, the hydrolysates were dialyzed against

102 distilled water for 48 h (molecular weight cut-off 3500). The solutions collected from both the inner

103 and outside fractions of dialysis bag were concentrated and lyophilized, named as 0.5h-I/O, 1h-I/O

4

104 and 2h-I/O, respectively.

2.4. Purity and molecular weight distribution

106 The purity and molecular weight distribution of the polysaccharide and its hydrolysates were

107 determined by HPSEC (Shimadzu SCL-10Avp, Shimadzu Scientific Instruments Inc., Columbia,

108 MA, USA) with multiple detectors: a differential pressure viscometer (DP), a refractive index

109 detector (RI), a UV detector, a right angle laser light scattering detector (RALLS) and a low angle

110 laser light scattering detector (LALLS). Two columns in series, a PAA-M (Aqua Gel^{TM} Series,

111 Polyanalytik Canada) and a PAA-203 (Aqua Gel^{TM} Series, Polyanalytik Canada) were used. The

112 eluent was 0.1 mol·L^{-1} NaNO$_3$/0.02% NaN$_3$ aqueous solution at a flow rate of 0.5 mL/min. The

113 temperature of columns, viscometers and RI detector was kept at 40 ºC. The dn/dc value was 0.146

114 mL/g. Polysaccharide and standard solutions were filtered through 0.45 μm filter prior to injection.

115 Data was obtained and processed using the OmniSEC 4.6.1 software.

2.5. Monosaccharide composition

117 Monosaccharide composition of polysaccharides was determined by a complete-acid hydrolyzing

118 in 2 mol·L^{-1} H$_2$SO$_4$ at 100 ºC   for 2 h, followed by high performance anion exchange

119 chromatography coupled with pulsed amperometric detection (HPAEC-PAD). Analysis of the

120 polysaccharide was performed on Dionex ICS-5000 System (Dionex Corporation, CA) equipped

121 with a CarboPac PA20 Guard (3 mm × 30 mm, Dionex, CA) and a CarboPac PA20 column (3

122 mm×150 mm, Dionex, CA), and separation was carried out under a gradient elution (2 mmol·L^{-1}

123 NaOH eluted for 20 min, followed by adding NaOAc from 5% to 20% in 10 min) at a flow rate of

124 0.5 mL/min. On the other hand, measurements of the polysaccharide and its hydrolysates were

125 recorded on Dionex ICS-500 System (Dionex Corporation, CA) fitted with a CarboPac PA1 column

126 (3 mm×150 mm, Dionex, CA) using a separation condition reported by Nie, et al. (2011).

2.6. Glyosidic linkages

128 Methylation analysis was carried out according to the method of Ciucanu and Kerek (1984) with

129 slight modification. Briefly, dried polysaccharide was stirred constantly overnight to make it

130 completely dissolve in anhydrous DMSO. Subsequently, prior to reacting with methyl iodide, dried

131 NaOH powder was added to make the polysaccharide solution in an alkaline environment. The

132 methylated polysaccharide was obtained by extracting with dichloromethane and further detected

133   by infrared spectra to confirm a complete reaction. The dried methylated product was hydrolyzed

134   by 4 mol·L^{-1} trifluoroacetic acid (TFA) in a sealed tube at 100 ºC for 6 h. Finally, the hydrolysate

135   was reduced with NaBD$_4$ and acetylated with acetic anhydride to result partially methylated alditol

136   acetates (PMAAs). The PMAAs were injected to a GC-MS system (Thermo 1310 GC-ISQ LT MS,)

137   with a TG-5MS capillary column (60 m×0.25 mm, 0.25 µm film thickness, 160 ºC to 210 ºC at 2 ºC

138   / min, then 210 ºC -240 ºC at 5 ºC / min) for analysis.

139   2.7.   NMR spectroscopy

140   The galactomannan and its hydrolysate (2h-I) was exchanged with deuterium by lyophilizing

141   against D$_2$O for three times and was finally dissolved in 0.7 mL D$_2$O, respectively, at room

142   temperature before NMR analysis.

143   For analysis of the galactomannan, studies included ^{1}H, ^{13}C spectrum, correlation spectroscopy

144   (COSY), heteronuclear single-quantum coherence (HSQC) and heteronuclear multiple-bond

145   correlation (HMBC), and were conducted at 294 K. And for analysis of the hydrolysate (2h-I), all

146   the experiments, including ^{1}H, ^{13}C spectrum, homonuclear ^{1}H/^{1}H correlation (COSY, TOCSY and

147   NOESY), HSQC and HMBC were carried out at 313K. All experiments were recorded on a Bruker

148   Avance 600 MHz NMR spectrometer (Brucker, Rheinstetten, Germany).

149   2.8.   Statistical analysis

150   The data was obtained with triple replications and was presented in mean, and the statistical analysis

151   was performed through statistical software (SPSS, Version 17.0).

152   **3.   Results and Discussion**

153   3.1 Purification and molecular weight of the galactomannan

154   The crude polysaccharide was obtained from the dry water-insoluble residues of natural *C. sinensis*

155   by cold alkali extraction and ethanol precipitation with a yield of approximately 1.91% ± 0.06 (w/w)

156   of the total dried materials. Due to a high content of protein (39.11% ±0.17) as determined by total

157   protein assay kit (Sigma-Aldrich, USA), it was then removed the protein by Sevag method and

158   protease hydrolysis before processing to ethanol precipitation.

159   The molecular weight distribution of the galactomannan was determined by HPSEC. As shown in

160   **Fig. 1b**, the galactomannan was eluted as a major and symmetrical peak from HPSEC, indicating

161   that this galactomannan was a homogeneous polysaccharide. The molecular weight (Mw) of the

162 galactomannan was calculated to be 7207 using pullulan as standard. Mw/Mn was used to

163 investigate the width of the molecular weight distribution, representing the dispersity of a polymer.

164 The Mw/Mn for the galactomannan was estimated to be 1.2, indicating that the polysaccharide was

165 a narrow-distributed polymer. The intrinsic viscosity of the polysaccharide was determined to be

166 0.032 dL/g, and the extreme low intrinsic viscosity might be attributed to its low molecular weight.

167 3.2 Partial acid hydrolysis and monosaccharide composition

168 The result of HPAEC-PAD analysis showed that the polysaccharide was mainly composed of

169 galactose, glucose and mannose in an approximate percentage of 68.65%, 6.65% and 24.02%, with

170 trace amount of rhamnose. The small amount of glucose might be the contamination of the water-

171 extracted polysaccharide, which was found to be an α-,4-glucan (Wang, et al., 2017). In addition,

172 no uronic acid was observed as detected on Dionex ICS-5000 System separated by CarboPac PA20

173 column (Supplemental Figure 1), indicating that the polysaccharide was a neutral polysaccharide.

174 Due to the structural complexity of polysaccharides, a partial acid hydrolysis process was employed

175 to characterize the galactomannan. **Fig. 1b** showed the HPSEC elution profiles of the hydrolysates

176 (the high molecular weight fragments) of the galactomannan. All the three fragments exhibited a

177 major sharp and symmetrical peak similar to the galactomannan, demonstrating that the hydrolysis

178 processes did not break up the main chain. It was worth noting that the retention volumes of the

179 hydrolysates were increased gradually with the increase of hydrolysis duration. Generally, it was

180 believed that the removal of branches was relative easier than that of the backbone of the

181 polysaccharide during the acid hydrolysis, since the acid prior to break up the residues in the side

182 chain or terminal of the polysaccharide. The increased of retention volumes suggested the effective

183 removal of side chains without a significant influence on backbone of the galactomannan. On the

184 other hand, it was interesting to find that the content of galactose in the inner side of dialysis bag

185 corresponding to the relative high molecular weight fragment was significantly decreased to 22.17%,

186 and further dropped to only around 2-3% as the hydrolysis duration extended to 1 h and 2 h (Table

187 1), indicating that the majority of galactose could be easily hydrolyzed by 0.1 M TFA. On the

188 contrary, the percentage of mannose was increased dramatically to 70.66%, 89.66% and 82.22%

189 after TFA treatment for 0.5 h, 1 h and 2 h, respectively. Unexpectedly, the result indicated that the

190 mannose, instead of galactose, was likely to locate in the backbone of the galactomannan, while

7

191   most of the galactose might exist in the branches.

192   3.3 Methylation analysis

193   Further detailed information of glycosidic linkages for the galactomannan and its hydrolysate (2h-

194   I) was investigated using methylation analysis coupled with GC-MS detection. Result suggested a

195   fairly complex structure with around 15 types of linkage patterns (**Table 2**, listed in the order of

196   retention time). Sugar residues, such as T-Gal*f*, 1,5-Gal*f*, 1,6-Man*p*, 1,6-Gal*f* and 1,2,6-Man*p*, were

197   the major residues in the galactomannan. However, the percentages of T-Gal*f*, 1,5-Gal*f* and 1,6-Gal*f*

198   were decreased significantly in the hydrolysate (2h-I), indicating these galactofuranosyl residues

199   were easily to move away by the acid and thus might be located at the end of branches. On the

200   contrary, 1,6-Man*p* increased dramatically to become the dominate sugar residue in the hydrolysate

201   (2h-I), accounting for 51.98% of all the linkage patterns.

202   Degree of branching (DB) is an important parameter that reflects the structure of a polymer. If the

203   value of DB equals to 0, it indicates that the polymer has a linear chain without any branches, but

204   for a fully branched structure, the number is 1 (Guo, et al., 2015). The DB for the galactomannan

205   and its hydrolysate (2h-I) was calculated to be 0.55 and 0.34, respectively, according to equation

206   reported by (Qian, Cui, Nikiforuk, & Goff, 2012), suggesting that the galactomannan had a highly

207   branched structure, but less branched after partial acid hydrolysis. Therefore, combined with the

208   results of monosaccharide composition and methylation analysis, we deduced that the main chain

209   of the galactomannan might be composed of 1,6-Man*p* mainly branching at O-2, and the terminal

210   sugar residues might be including T-Gal*f*, T-Man*p*, as well as the small percentage of T-Glc*p* and T-

211   Gal*p*.

212   3.4 NMR spectroscopy analysis of the galactomannan

213   The ^{1}H NMR spectrum (**Fig. 2a**) of the galactomannan showed a complex pattern of signals in the

214   anomeric region, since more than ten peaks were detected. Among them, three major (5.15, 4.96

215   and 4.94 ppm) and four minor (5.07, 5.06, 4.99 and 4.83 ppm) anomeric signals were found to be

216   significant and were used for analysis. In ^{13}C NMR spectrum (**Fig. 2b**), the dominant anomeric

217   signals were centered at 108.12 ppm and 107.26 ppm, indicating the presence of β-galactofuranosyl

218   residues because of the obvious low field. Meanwhile, six minor peaks (106.13, 101.24, 100.84,

219   99.84, 98.38 and 97.35 ppm) were also observed. From the HSQC spectrum (**Fig. 2d**), nine peaks

220   were clearly determined which were labeled A-I according to the chemical shift of their anomeric

221   protons. The COSY, HSQC and HMBC experiments allowed partial assignment of the nine residues,

222   and the result was shown in **Table 3**.

223   The intensive anomeric signals of **residue A** appeared at 5.15 ppm and 107.26 ppm, indicating a β-

224   configuration of Gal$f$ unit that had a relative high content in the galactomannan. The proton

225   assignment of residue A (From H-2 to H-6/6': 4.08, 3.99, 4.00, 3.90 and 3.81/3.56 ppm) was

226   obtained from COSY spectrum (**Fig. 2c**). The corresponding chemical shifts of carbon were 81.52,

227   76.96, 83.16, 69.89 and 69.52 ppm for C-2, C-3, C-4, C-5 and C-6, respectively, as revealed by

228   HSQC spectrum (**Fig. 2d**). The downfield shift of C-6 led to the identification of residue A as β-1,6-

229   Gal$f$. On the other hand, the **residue C**, which had H-1 and C-1 of 5.06 ppm and 106.13 ppm, was

230   also endorsed as β-1,6-Gal$f$ unit. The slight difference of chemical shifts for the 6-O substituted β-

231   Gal$f$ residues indicated the location of different chemical environments. The assignment of these

232   two residues was also confirmed by comparing with the value from literatures (Bernabé, Salvachúa,

233   Jiménez-Barbero, Leal, & Prieto, 2011; Bi, et al., 2013; Górska-Frączek, et al., 2011; Prieto, et al.,

234   1997).

235   A complete assignment of signals derived from **residue F** and **G** was successfully achieved, as

236   shown in **Fig. 2c** and **Table 3**. The β-configuration form of both residues was established by

237   chemical shifts at 4.96 ppm (**residue F**) and 4.94 ppm (**residue G**) of H-1, as well as 108.12 ppm

238   of C-1. The obvious downfield shift of C-5 of residue G (**Fig. 2d**), in addition to result from

239   methylation analysis, allowed assigning residue G to β-1,5-Gal$f$. The residue F, on the other hand,

240   without any ^{13}C shifts induced by glycosylation, was deduced to β-T-Gal$f$. Besides, both of the

241   residues possessed all typical chemical shifts in comparison of the observed values with those

242   reported in the literatures (Ahrazem, Leal, Prieto, Jiménez-Barbero, & Bernabé, 2001; Bernabé, et

243   al., 2011; Giménez-Abián, Bernabé, Leal, Jiménez-Barbero, & Prieto, 2007; J. Leal, Jiménez-
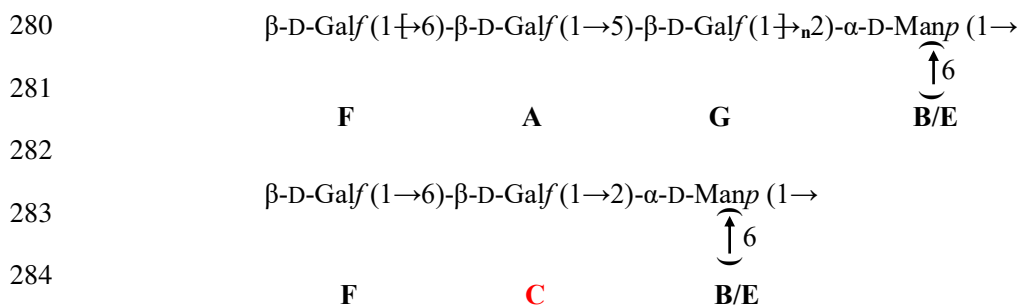
244   Barbero, Bernabé, & Prieto, 2008).

245   The anomeric chemical shift for **residue D** was 4.99/98.38 ppm, suggesting that it was an α-linked

246   unit. The chemical shifts for the H2-6/6' of residue D were identified as 3.53, 3.64, 3.44, 3.62 and

247   3.82/3.72, respectively, by the well-resolved cross-peaks in the COSY spectrum, and the

248   corresponding ^{13}C signals were identified from the HSQC spectrum. Comparing the chemical shifts

249 with the previous studies (Chen, Zhang, Chen, & Cheung, 2014; Guo, et al., 2012), for both protons

250 and carbons, allowed to deduce residue D as α-T-Glc*p*.

251 However, the information for the other residues was poor due to overlapping of signals, both for [1]H

252 and ^{13}C spectra, especially for the residue B, E and H. The anomeric signal of **residue B, E and H**

253 was 5.15/101.24, 4.96/97.35 and 5.07/100.84 ppm, respectively. Through COSY spectrum (**Fig. 2c**),

254 the chemical shift of H-2 was determined at 4.04, 4.04 and 4.08 ppm for residue B, E and H,

255 respectively. Therefore, the corresponding C-2 chemical shift was figured out at 76.96, 76.96 and

256 76.61 ppm, respectively, by HSQC spectrum. The downfield shift of C-2s suggested that all the

257 three residues carried a 2-O-subsituted carbon. Besides, the result from methylation analysis had

258 evidenced the presence of 1,2-Man*p*, 1,2,6-Man*p* and 1,2,4,6-Man*p*. By comparison of the chemical

259 shifts with those of previous reports (Omarsdottir, et al., 2006) and consideration of the methylation

260 result, the residue B, E and H was deduced to α-1,2-Man*p*, α-1,2,6-Man*p* and α-1,2,4,6-Man*p*,

261 respectively. With regard to residue I, the weak coupling between H-1 and H-2 precluded the

262 discrimination and assignation of cross peaks. This assignment, however, was partially achieved in

263 the current study by comparing the chemical shifts with literatures figures (Bernabé, et al., 2011;

264 Jiménez-Barbero, Prieto, Gómez-Miranda, Leal, & Bernabé, 1995) and analyzing the cross peaks

265 in the HSQC spectrum, thus contributing to identify **residue I** as α-1,6-Man*p*.

266 A long-range HMBC spectroscopy was employed to identify the sequences between glycosyl

267 residues, as shown in **Fig. 2e** and summarized in **Table 3**. Cross-peaks of both anomeric protons

268 and carbons of each glycosyl residue were examined. Cross-peaks were found between H-1 (5.15

269 ppm) of residue A and C-5 (75.91 ppm) of residue G (**A H-1, G C-5**); C-1 (107.26 ppm) of residue

270 A and H-5 (3.89 ppm) of residue G (**A C-1, G H-5**). Similarly, cross-peaks between H-1 (4.96 ppm)

271 of residue F and C-6 (69.52 ppm) of residue A (**F H-1, A C-6**); cross-peaks between H-1 (4.94 ppm)

272 of residue G and C-6 (69.52 ppm) of residue A (**G H-1, A C-6**); C-1 (108.12 ppm) of residue F/G

273 and H-6/6' (3.56, 3.81 ppm) of residue A (**F/G C-1, A H-6/6'**) were observed.   Cross-peaks

274 between H-1 (4.94 ppm) of residue G and C-2 (76.69 ppm) of residue B/E (**G H-1, B/E C-2**), as

275 well as C-1 (108.13 ppm) of residue G and H-2 (4.04 ppm) of residue B/E (**G C-1, B/E H-2**) were

276 found. Likewise, weak cross-peaks between H-1 (5.06 ppm) of residue C and C-2 (76.96 ppm) of

277 residue B/E (**C H-1, B/E C-2**); C-1 (106.13 ppm) of residue C and H-2 (4.04 ppm) of residue B/E

278 (**C C-1, B/E H-2**) were observed. Combining the above result, the following possible fragments of

279 sequences in the galactomannan would be concluded:

280 β-D-Gal*f* (1⤳6)-β-D-Gal*f* (1→5)-β-D-Gal*f* (1⟩$_n$2)-α-D-Man*p* (1→

281 ↑6

282 **F** **A** **G** **B/E**

283 β-D-Gal*f* (1→6)-β-D-Gal*f* (1→2)-α-D-Man*p* (1→

284 ↑6

F **C** **B/E**

285 However, the correlations of the other sugar residues, especially those among residues B, E, H and

286 I, were not unambiguous detected due to their low resonance signal intensity. As a result, not much

287 information could be drawn through the current NMR experiments for the mannan core. Therefore,

288 the NMR analysis for the hydrolysate (2h-I) was conducted to get the information of the

289 mannopyranoses.

290 3.5 NMR spectroscopy analysis of the hydrolysate (2h-I)

291 In order to investigate the additional connections among these residues, a mild acid hydrolysis

292 experiment was carried out to selectively hydrolyze the polysaccharide, taking the advantage of the

293 lability of the glycosidic linkages of the furanoid rings, compared with that of the mannan pyranoid

294 rings. Treatment with 0.1 TFA for 2 h at 100 ˚C removed the majority of the Gal*f* moiety as supported

295 by the monosaccharide composition and methylation results. Therefore, 1D and 2D NMR spectra

296 were further conducted for the hydrolysate (2h-I) to provide more detailed structural information of

297 the main chain. The peaks in the anomeric region were designated **J** (4.82/99.31 ppm), **K**

298 (5.16/100.67 ppm), **L** (5.14/100.61 ppm), **M** (5.03/98.16 ppm), **N** (4.96/102.22 ppm) and **O**

299 (5.04/105.78 ppm), as marked in **Fig. 3a and 3b**. The ^{1}H and ^{13}C signals were assigned using COSY,

300 TOCSY, HSQC, HMBC and NOESY spectrum, which were listed in **Table 4**.

301 **Residue J** showed the dominant intensity both in the ^{1}H and ^{13}C spectrum, and was tentatively

302 assigned to α-1,6-Man*p*. The chemical shifts of H-1, H-2, H-3, H-4, H-5 and H6/6' were

303 successfully obtained from the COSY spectrum (**Fig. 3c**), which was 4.82, 3.91, 3.75, 3.65, 3.78

304 and 3.71/3.86, respectively. Additionally, following the dotted **J** line marked in the TOCSY

305 spectrum (**Fig. 3d**), five signals at 3.91, 3.86, 3.78, 3.75 and 3.65 ppm were clearly observed,

306 matched well with the chemical shifts from COSY spectrum, except for the signals of 3.71 ppm due

11

307   to the overlapping. The chemical shifts for C-1 to C-6 of this residue were demonstrated to be 99.31,

308   69.91, 70.67, 66.53, 70.64 and 65.43 ppm based on the cross-peaks in the HSQC spectrum (**Fig. 3e**).

309   The assignment was in accordance with the values reported by the literature (Bernabé, et al., 2011;

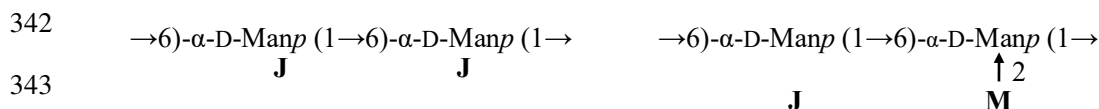310   Bi, et al., 2011; Jiménez-Barbero, et al., 1995).

311   In the HSQC spectrum, the anomeric proton signals at δ 5.16 ppm (**residue K**) and 5.14 ppm

312   (**residue L**) that correlated with the anomeric carbon signal at δ 100.67 ppm and δ 100.61 ppm,

313   respectively, were both endorsed as α-1,2-Man*p*. According to COSY spectrum, the H-2, H-3 and

314   H-4 were determined at 4.03, 3.88 and 3.69 ppm for residue K, and 4.02, 3.87 and 3.66 ppm for

315   residue L, respectively. Due to the severe crowding and low intensity of the cross peaks, it was

316   difficult to achieve an unambiguous assignment of all the signals. This issue, however, was

317   addressed by examining the cross peaks through TOCSY and HSQC spectrum (**Fig. 3d and 3e**),

318   together with comparing the data from the previous reports (Molinaro, Piscopo, Lanzetta, & Parrilli,

319   2002; Omarsdottir, et al., 2006). The full assignment of ^{1}H and ^{13}C was also obtained and was

320   summarized in **Table 4**.

321   The cross peak at 5.03/98.16 ppm in the anomeric region of HSQC spectrum was tentatively

322   assigned to α-1,2,6-Man*p* (**residue M**). The chemical shifts of H-2 (3.95 ppm), H-3 (3.89 ppm) and

323   H-4 (3.61 ppm) was achieved by the well-resolved cross peaks in the COSY spectrum (**Fig. 3c**), and

324   was also confirmed in the TOCSY spectrum (**Fig. 3d,** Line M). But the chemical shifts of H-5 and

325   H-6/6' were unobtainable because of the relative low abundance and high degree of signal

326   overlapping due to the structural similarity. The assignment of some peaks was derived from HSQC

327   spectroscopy, and meantime the corresponding chemical shifts of carbon were also identified from

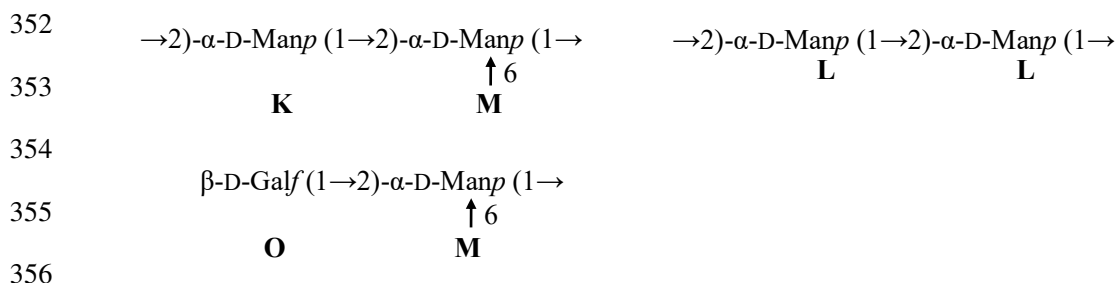328   that spectrum, as listed in **Table 4**.

329   The chemical shift of ^{1}H at 4.96 ppm and ^{13}C at 102.22 ppm indicated that **residue N** should be

330   assigned to α-T-Man*p*. The chemical shifts for the H-1, H-2, H-3, H-4, H-5 and H-6/6' were

331   identified as 4.96, 3.99, 3.76, 3.57, 3.68 and 3.68/3.80 ppm, respectively, through COSY spectrum.

332   The corresponding chemical shifts for C-1 to C-6 were achieved in HSQC spectrum, and the result

333   was in consistence with the literature values (Molinaro, et al., 2002; Omarsdottir, et al., 2006), which

334   confirmed the assignment of residue N.

335   Examining the cross-peaks of both the anomeric proton and carbon in the HMBC spectrum, the
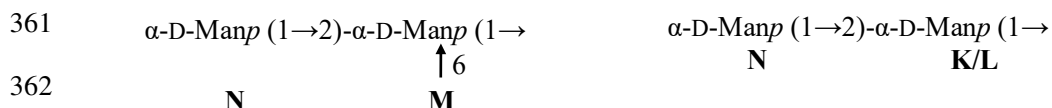
sequence of glycosyl residues of this polysaccharide was evidenced (**Fig. 3f**). Obviously, residue J

correlated with two sugar residues both at C-6 and H-6, residue J (**J H-1, J C-6; J C-1, J H-6/6'**)

and residue M (**J H-1, M C-6; J C-1, M H-6/6'**). Besides, cross-peaks between H-1 (5.03 ppm) of

residue M and C-6 (65.43 ppm) of residue J (**M H-1, J C-6**); C-1 (98.16 ppm) of residue M and H-

6 (3.86 ppm) of residue J (**M C-1, J H-6**) was also found. Thus, the following sequences were

established:

$$\to 6)\text{-}\alpha\text{-}D\text{-}Man}p\ (1\to 6)\text{-}\alpha\text{-}D\text{-}Man}p\ (1\to \qquad \to 6)\text{-}\alpha\text{-}D\text{-}Man}p\ (1\to 6)\text{-}\alpha\text{-}D\text{-}Man}p\ (1\to$$

$$\text{J} \qquad\qquad \text{J} \qquad\qquad\qquad\qquad \uparrow 2$$

$$\text{J} \qquad\qquad \text{M}$$

In addition, cross-peaks between the H-1 (5.16 ppm) of residue K and C-2 (78.63 ppm) of residue

M (**K H-1, M C-2**); C-1 (100.67 ppm) of residue K and H-2 (3.95 ppm) of residue M (**K C-1, M**

H-2); H-1 (5.14 ppm) of residue L and C-2 (78.09 ppm) of residue L (**L H-1, L C-2**); C-1 (100.61

ppm) of residue L and H-2 (4.02 ppm) of residue L (**L C-1, L H-2**) was observed. Besides, cross-

peak between H-1 (5.04 ppm) of residue O and C-2 (78.63 ppm) of residue M (**O H-1, M C-2**) was

also clearly evidenced. And this cross-peak suggested that the remaining small percentage of β-D-

Gal*f* was directly linked to the backbone at O-2 of α-1,2,6-Man*p*. The following sequences were

therefore indicated:

$$\to 2)\text{-}\alpha\text{-}D\text{-}Man}p\ (1\to 2)\text{-}\alpha\text{-}D\text{-}Man}p\ (1\to \qquad \to 2)\text{-}\alpha\text{-}D\text{-}Man}p\ (1\to 2)\text{-}\alpha\text{-}D\text{-}Man}p\ (1\to$$

$$\uparrow 6 \qquad\qquad\qquad\qquad \text{L} \qquad\qquad \text{L}$$

$$\text{K} \qquad\qquad \text{M}$$

$$\beta\text{-}D\text{-}Gal}f\ (1\to 2)\text{-}\alpha\text{-}D\text{-}Man}p\ (1\to$$

$$\uparrow 6$$

$$\text{O} \qquad\qquad \text{M}$$

With regard to residue N, the H-1 (4.96 ppm) correlated with C-2 (78.09 ppm) of residue K/L (**N**

H-1, K/L C-2) and C-2 (78.63 ppm) of residue M (**N H-1, M C-2**), and the C-1 (102.22 ppm)

showed obviously cross-peak with H-2 (4.03 ppm) of residue K (**N C-1, K H-2**) and H-2 (4.02 ppm)

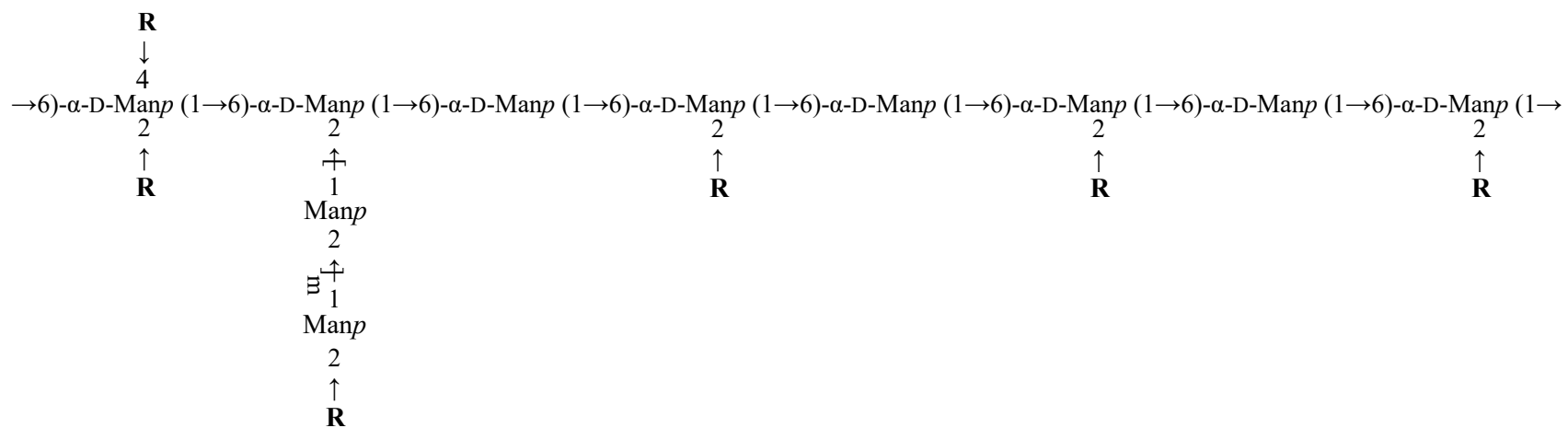of residue L (**N C-1, L H-2**), suggesting the presence of the following sequences:

$$\alpha\text{-}D\text{-}Man}p\ (1\to 2)\text{-}\alpha\text{-}D\text{-}Man}p\ (1\to \qquad \alpha\text{-}D\text{-}Man}p\ (1\to 2)\text{-}\alpha\text{-}D\text{-}Man}p\ (1\to$$

$$\uparrow 6 \qquad\qquad\qquad\qquad \text{N} \qquad\qquad \text{K/L}$$

$$\text{N} \qquad\qquad \text{M}$$

NOESY spectroscopy correlates nuclei through space, so both the inter- and intra-residual

connectivities could be observed, which not only confirmed the assignments of chemical shifts for

365 the illustrated sugar residues, but demonstrated the aforementioned sequences of glycosidic linkages,

366 as shown in **Fig. 3g**.

367 Although the linkage information of α-1,2,4,6-Man*p* residue was not sufficient enough from the

368 above NMR spectrums due to its relative low content and structural similarity, the methylation result

369 together with monosaccharide composition deduced its presence in the main chain. A significant

370 decrease of the content was observed after treating with mild acid, suggesting the branches that

371 linked to α-1,2,4,6-Man*p* were probably Gal*f* chains.

372 Combined all the data from the galactomannan and its hydrolysate (2h-I), the idealized structure of

373 the polysaccharide was proposed to be:

374

```
                          R
                          ↓
                          4
→6)-α-D-Manp (1→6)-α-D-Manp (1→6)-α-D-Manp (1→6)-α-D-Manp (1→6)-α-D-Manp (1→6)-α-D-Manp (1→6)-α-D-Manp (1→6)-α-D-Manp (1→
        2                 2                                   2                 2                                   2
        ↑                 ↑                                   ↑                 ↑                                   ↑
        R                 1                                   R                 R                                   R
                         Manp
                          2
                          ↑
                        m 1
                         Manp
                          2
                          ↑
                          R
```

375

376

377 **m** might be 0, 1 or 2.

378 **R** could be as follows:

379 β-D-Galf (1→6)-β-D-Galf (1→5)-β-D-Galf (1→)$_n$ (major), **n** might be 1 or 2;   β-D-Galf (1→6)-β-D-Galf (1→ (minor);

380

381

382

4. Conclusion

In the present study, a novel α-1,6-linked galactomannan was obtained from water-insoluble residues of natural *C. sinensis* through alkali extraction. The Mw and intrinsic viscosity of this galactomannan was 7207 and 0.032 dL/g, respectively, and it was composed of galactose, glucose and mannose in a percentage of 68.65%, 6.65% and 24.02%, with trace amount of rhamnose. The backbone of this galactomannan was made up of linear α-1,6-Man*p*. The major branches, composed of β-1,6-Gal*f* and β-1,5-Gal*f*, were linked to *O*-2 and *O*-4 of the backbone. Another kind of branch was composed of β-1,6-Gal*f* and β-1,5-Gal*f* linking to the C-2 of α-1,2-Man*p* residues attaching to the main chain. All the branches were terminated at β-T-Gal*f*. The possible structure of this novel galactomannan was established. This study provided substantial updated structural information for the polysaccharide from *C. sinensis*.

References

Ahrazem, O., Leal, J., Prieto, A., Jiménez-Barbero, J., & Bernabé, M. (2001). Chemical structure of a polysaccharide isolated from the cell wall of *Arachniotus verruculosus* and *A. ruber*. *Carbohydrate Research, 336*(4), 325-328.

Bernabé, M., Salvachúa, D., Jiménez-Barbero, J., Leal, J. A., & Prieto, A. (2011). Structures of wall heterogalactomannans isolated from three genera of entomopathogenic fungi. *Fungal Biology, 115*(9), 862-870.

Bi, H., Gao, T., Li, Z., Ji, L., Yang, W., Iteku, B. J., et al. (2013). Structural elucidation and antioxidant

415　　　　activity of a water-soluble polysaccharide from the fruit bodies of *Bulgaria inquinans* (Fries).
416　　　　*Food Chemistry, 138*(2), 1470-1475.

417　Bi, H., Han, H., Li, Z., Ni, W., Chen, Y., Zhu, J., et al. (2011). A water-soluble polysaccharide from the
418　　　　fruit bodies of *Bulgaria inquinans* (Fries) and its anti-malarial activity. *Evidence-Based*
419　　　　*Complementary and Alternative Medicine, 2011*.

420　Chen, L., Zhang, B.-B., Chen, J.-L., & Cheung, P. C. (2014). Cell wall structure of mushroom sclerotium
421　　　　(*Pleurotus tuber-regium*): Part 2. Fine structure of a novel alkali-soluble hyper-branched cell
422　　　　wall polysaccharide. *Food Hydrocolloids, 38*, 48-55.

423　Chen, P. X., Wang, S., Nie, S., & Marcone, M. (2013). Properties of *Cordyceps sinensis*: A review.
424　　　　*Journal of Functional Foods, 5*(2), 550-569.

425　Ciucanu, I., & Kerek, F. (1984). A simple and rapid method for the permethylation of carbohydrates.
426　　　　*Carbohydrate Research, 131*(2), 209-217.

427　Górska-Frączek, S., Sandström, C., Kenne, L., Rybka, J., Strus, M., Heczko, P., et al. (2011). Structural
428　　　　studies of the exopolysaccharide consisting of a nonasaccharide repeating unit isolated from
429　　　　*Lactobacillus rhamnosus* KL37B. *Carbohydrate Research, 346*(18), 2926-2932.

430　Giménez-Abián, M. I., Bernabé, M., Leal, J. A., Jiménez-Barbero, J., & Prieto, A. (2007). Structure of a
431　　　　galactomannan isolated from the cell wall of the fungus *Lineolata rhizophorae. Carbohydrate*
432　　　　*Research, 342*(17), 2599-2603.

433　Guo, Q., Cui, S. W., Kang, J., Ding, H., Wang, Q., & Wang, C. (2015). Non-starch polysaccharides from
434　　　　American ginseng: physicochemical investigation and structural characterization. *Food*
435　　　　*Hydrocolloids, 44*, 320-327.

436　Guo, Q., Cui, S. W., Wang, Q., Hu, X., Kang, J., & Yada, R. Y. (2012). Structural characterization of a
437　　　　low-molecular-weight　heteropolysaccharide　(glucomannan)　isolated　from
438　　　　*Artemisiasphaerocephala Krasch. Carbohydrate research, 350*, 31-39.

439　Jiménez-Barbero, J., Prieto, A., Gómez-Miranda, B., Leal, J. A., & Bernabé, M. (1995). Chemical
440　　　　structure of fungal cell-wall polysaccharides isolated from *Microsporum gypseum* and related
441　　　　species of *Microsporum* and *Trychophyton. Carbohydrate Research, 272*(1), 121-128.

442　Kiho, T., Tabata, H., Ukai, S., & Hara, C. (1986). A minor, protein-containing galactomannan from a
443　　　　sodium carbonate extract of *Cordyceps sinensis. Carbohydrate Research, 156*, 189-197.

444　Leal, J., Jiménez-Barbero, J., Bernabé, M., & Prieto, A. (2008). Structural elucidation of a cell wall fungal
445　　　　polysaccharide isolated from *Ustilaginoidea virens*, a pathogenic fungus of *Oriza sativa* and
446　　　　*Zea mays. Carbohydrate Research, 343*(17), 2980-2984.

447　Leal, J. A., Prieto, A., Bernabé, M., & Hawksworth, D. L. (2010). An assessment of fungal wall
448　　　　heteromannans as a phylogenetically informative character in ascomycetes. *FEMS*
449　　　　*Microbiology Reviews, 34*(6), 986-1014.

450　Miyazaki, T., Oikawa, N., & Yamada, H. (1977). Studies on fungal polysaccharides. XX. Galactomannan
451　　　　of *Cordyceps sinensis. Chemical and Pharmaceutical Bulletin, 25*(12), 3324-3328.

452　Molinaro, A., Piscopo, V., Lanzetta, R., & Parrilli, M. (2002). Structural determination of the complex
453　　　　exopolysaccharide from the virulent strain of *Cryphonectria parasitica. Carbohydrate Research,*
454　　　　*337*(19), 1707-1713.

455　Nie, S.-P., Cui, S. W., Phillips, A. O., Xie, M.-Y., Phillips, G. O., Al-Assaf, S., et al. (2011). Elucidation
456　　　　of the structure of a bioactive hydrophilic polysaccharide from Cordyceps sinensis by
457　　　　methylation analysis and NMR spectroscopy. *Carbohydrate Polymers, 84*(3), 894-899.

458　Nie, S., Cui, S. W., Xie, M., Phillips, A. O., & Phillips, G. O. (2013). Bioactive polysaccharides from

459   *Cordyceps sinensis*: Isolation, structure features and bioactivities. *Bioactive Carbohydrates and*

460   *Dietary Fibre, 1*(1), 38-52.

461 Omarsdottir, S., Petersen, B., Barsett, H., Paulsen, B. S., Duus, J., & Olafsdottir, E. (2006). Structural

462   characterisation of a highly branched galactomannan from the lichen *Peltigera canina* by

463   methylation analysis and NMR-spectroscopy. *Carbohydrate Polymers, 63*(1), 54-60.

464 Omarsdottir, S., Petersen, B. O., Paulsen, B. S., Togola, A., Duus, J. Ø., & Olafsdottir, E. S. (2006).

465   Structural characterisation of novel lichen heteroglycans by NMR spectroscopy and methylation

466   analysis. *Carbohydrate Research, 341*(14), 2449-2455.

467 Prieto, A., Leal, J. A., Poveda, A., Jiménez-Barbero, J., Gómez-Miranda, B., Domenech, J., et al. (1997).

468   Structure of complex cell wall polysaccharides isolated from *Trichoderma* and *Hypocrea*

469   species. *Carbohydrate Research, 304*(3), 281-291.

470 Qian, K.Y., Cui, S. W., Nikiforuk, J., & Goff, H. D. (2012). Structural elucidation of

471   rhamnogalacturonans from flaxseed hulls. *Carbohydrate Research, 362*, 47-55.

472 Wang, J., Kan, L., Nie, S., Chen, H., Cui, S. W., Phillips, A. O., et al. (2015). A comparison of chemical

473   composition, bioactive components and antioxidant activity of natural and cultured *Cordyceps*

474   *sinensis*. *LWT-Food Science and Technology, 63*(1), 2-7.

475 Wang, J., Nie, S., Cui, S. W., Wang, Z., Phillips, A. O., Phillips, G. O., et al. (2017). Structural

476   characterization and immunostimulatory activity of a glucan from natural Cordyceps sinensis.

477   *Food Hydrocolloids*, *67*, 139-147.

478 Wang, J., Nie, S., Kan, L., Chen, H., Cui, S. W., Phillips, A. O., et al. (2017). Comparison of structural

479   features and antioxidant activity of polysaccharides from natural and cultured *Cordyceps*

480   *sinensis*. *Food Science and Biotechnology*, *26(1)*, 55-62.

481 Zhang, M., Cui, S., Cheung, P., & Wang, Q. (2007). Antitumor polysaccharides from mushrooms: a

482   review on their isolation process, structural characteristics and antitumor activity. *Trends in*

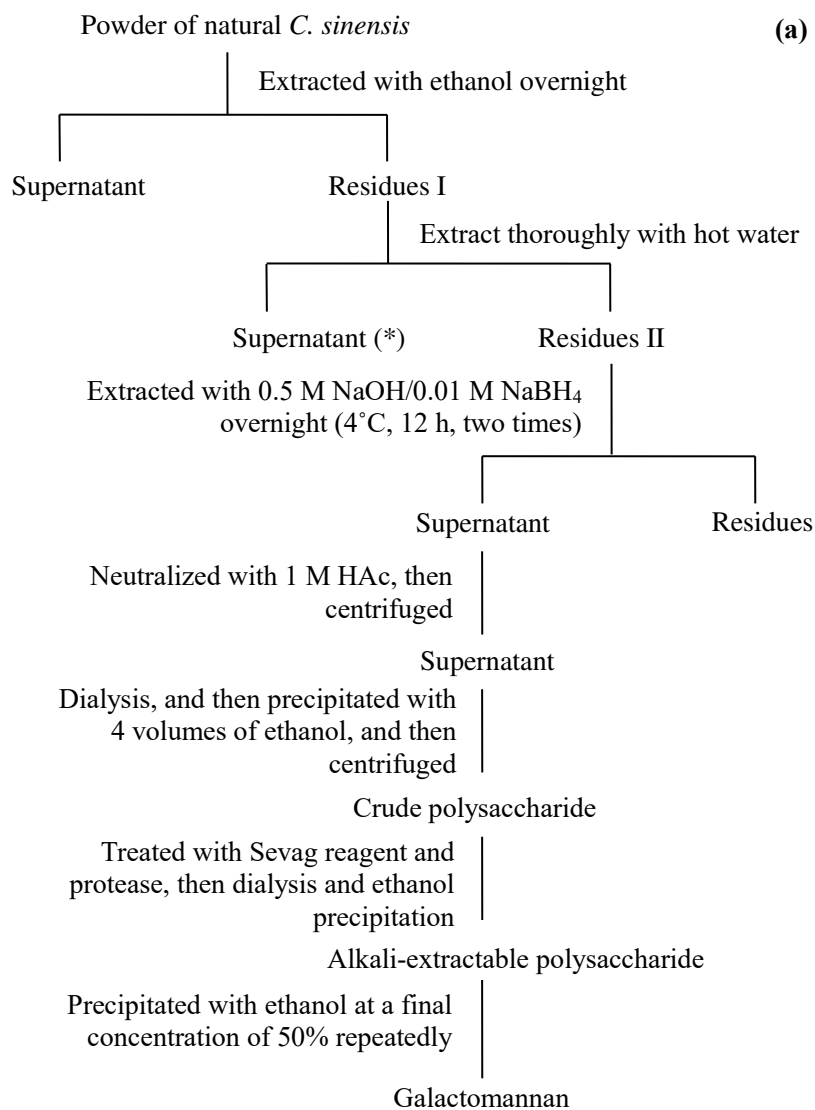483   *Food Science & Technology, 18*(1), 4-19.

484

485

486   **FIGURES**

487

488   **Figure 1**

Powder of natural *C. sinensis*   **(a)**

Extracted with ethanol overnight

Supernatant   Residues I

Extract thoroughly with hot water

Supernatant (*)   Residues II

Extracted with 0.5 M NaOH/0.01 M NaBH$_4$
overnight (4˚C, 12 h, two times)

Supernatant   Residues

Neutralized with 1 M HAc, then
centrifuged

Supernatant

Dialysis, and then precipitated with
4 volumes of ethanol, and then
centrifuged

Crude polysaccharide

Treated with Sevag reagent and
protease, then dialysis and ethanol
precipitation

Alkali-extractable polysaccharide

Precipitated with ethanol at a final
concentration of 50% repeatedly

Galactomannan

489

490   * This fraction was further isolated and purified to obtain the water-extracted polysaccharide, as

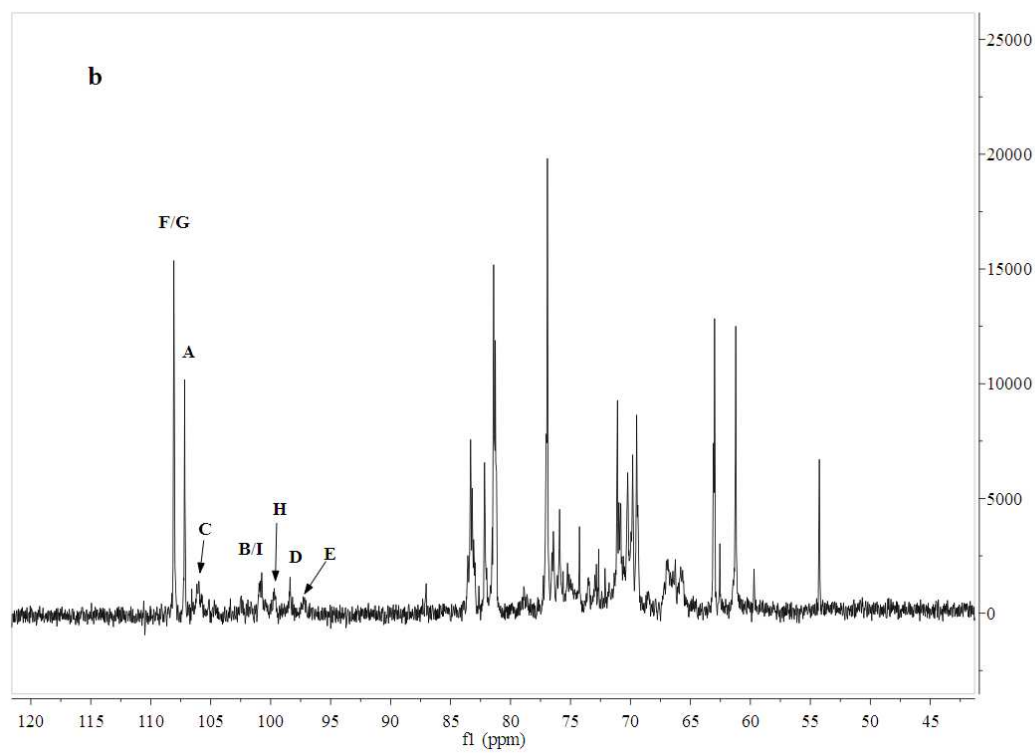491   described in our previous report (Wang, et al., submitted for publication)
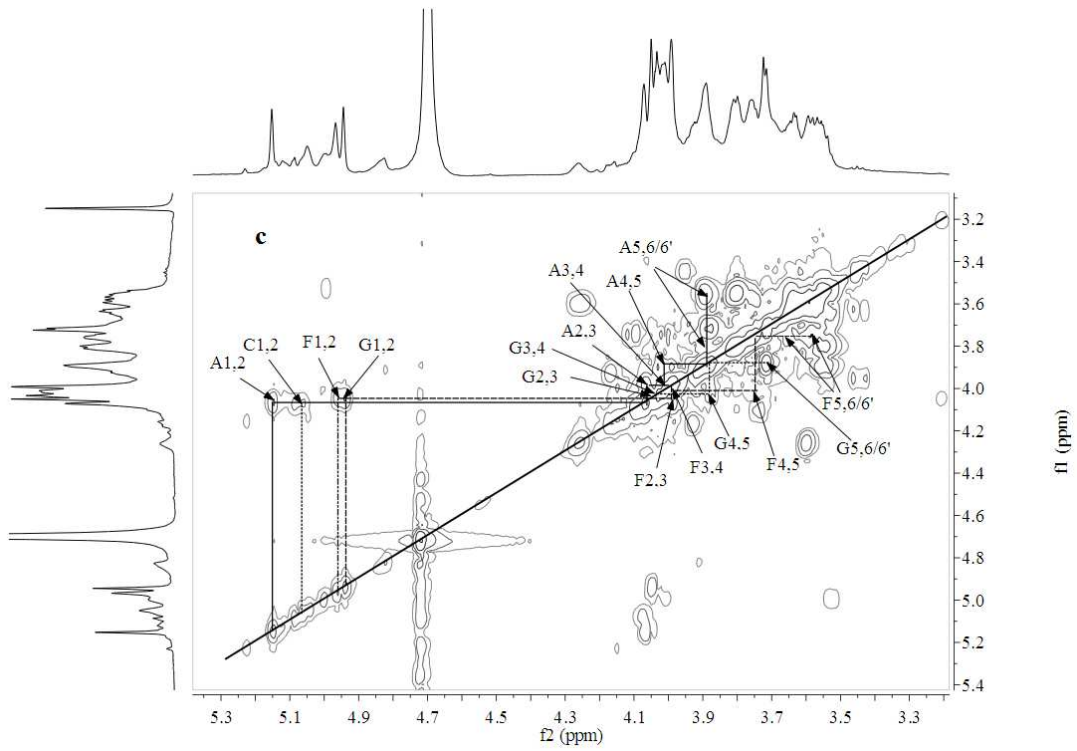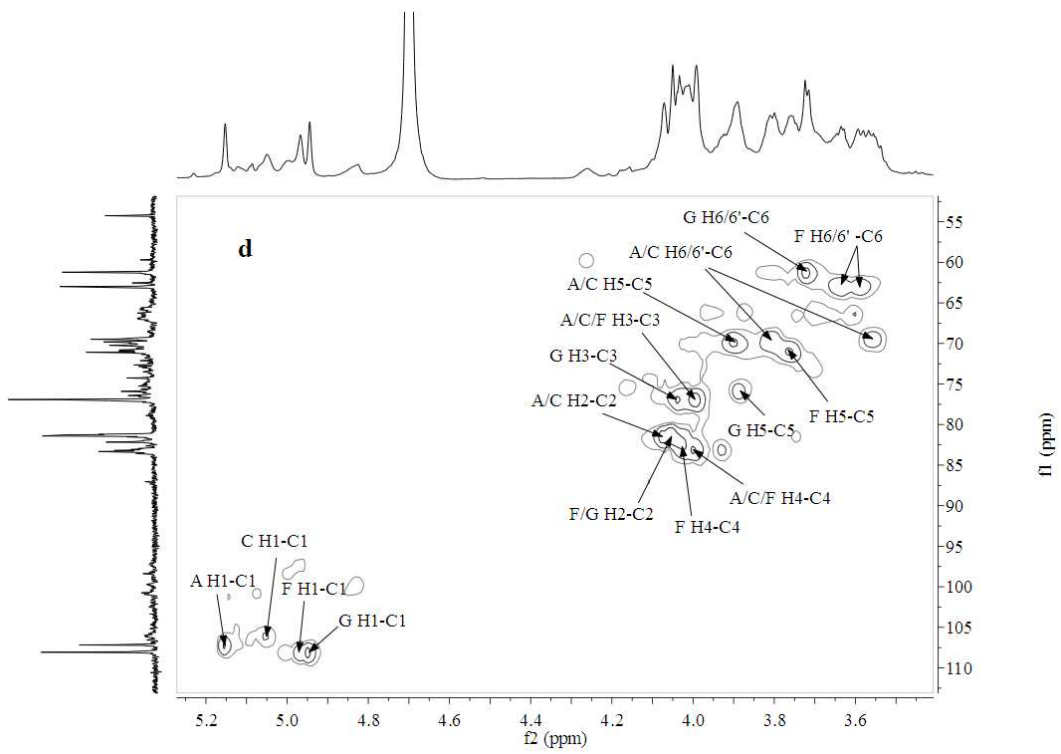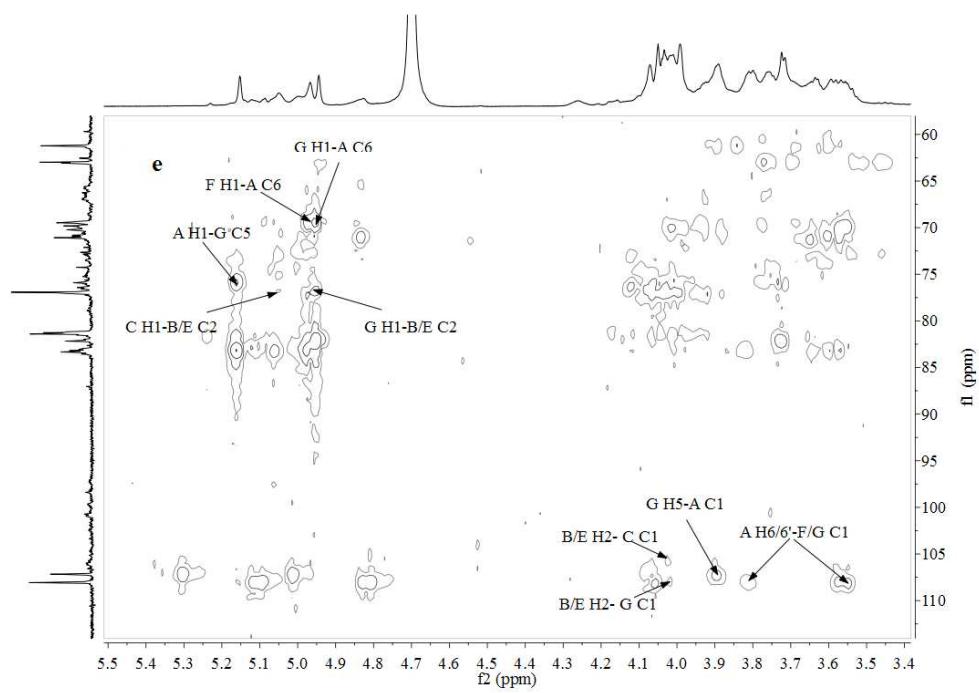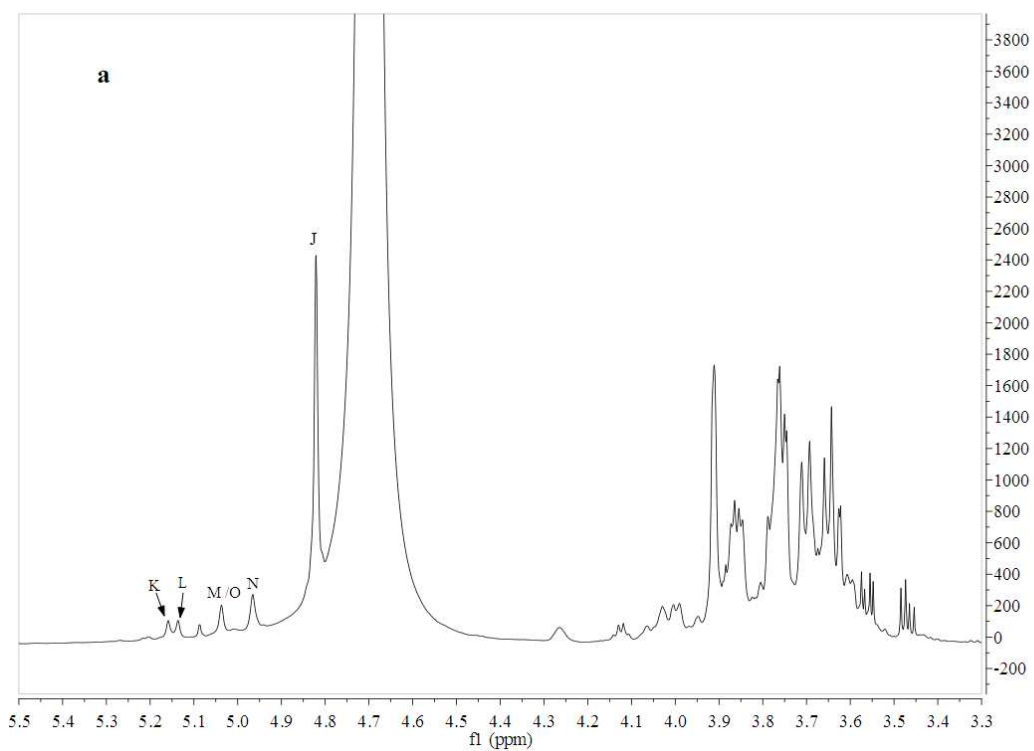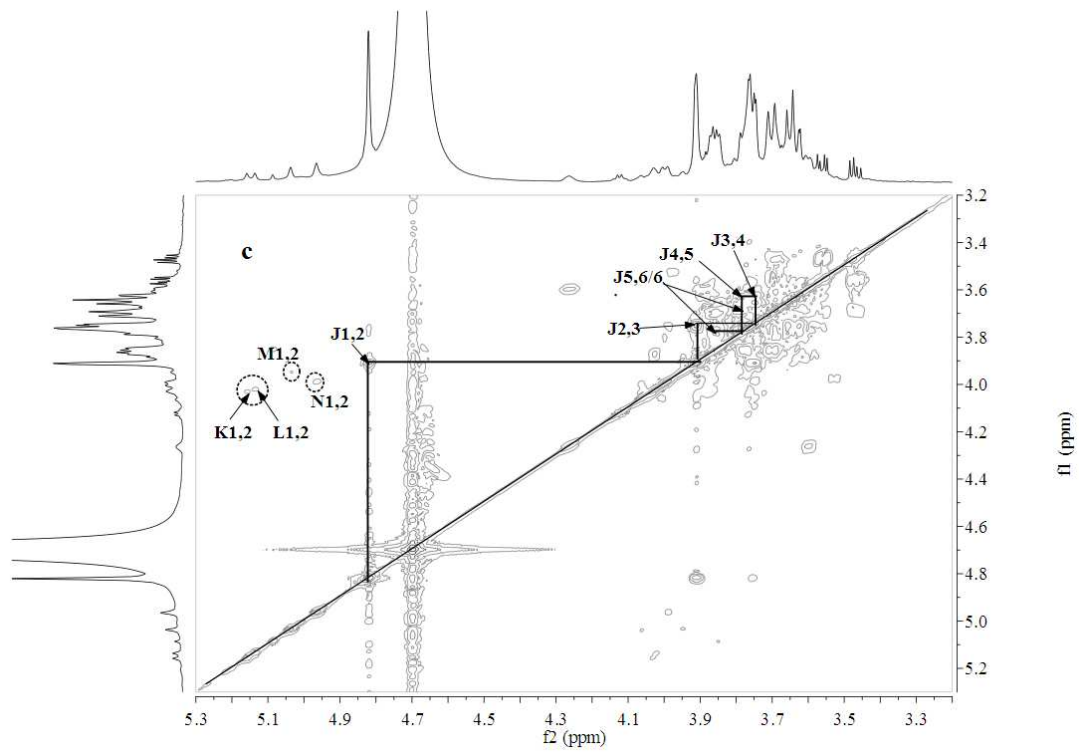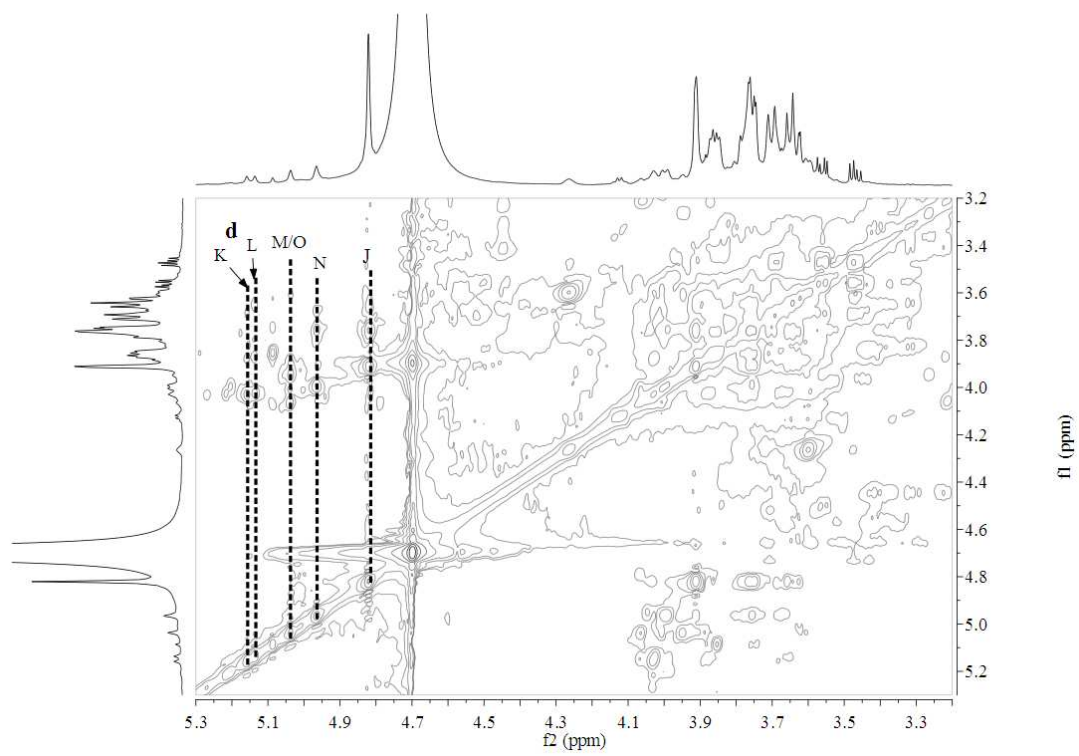
492
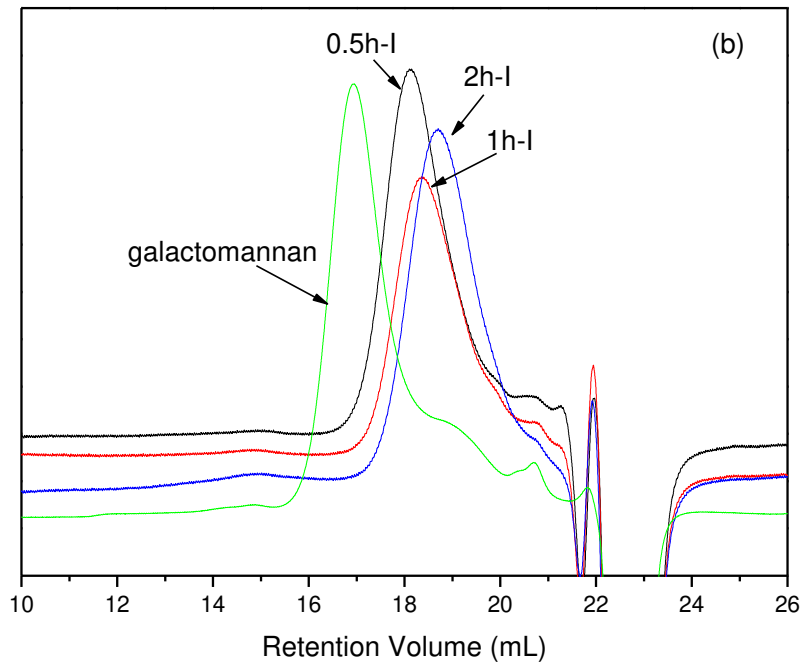
493

494

495 **Figure 2**
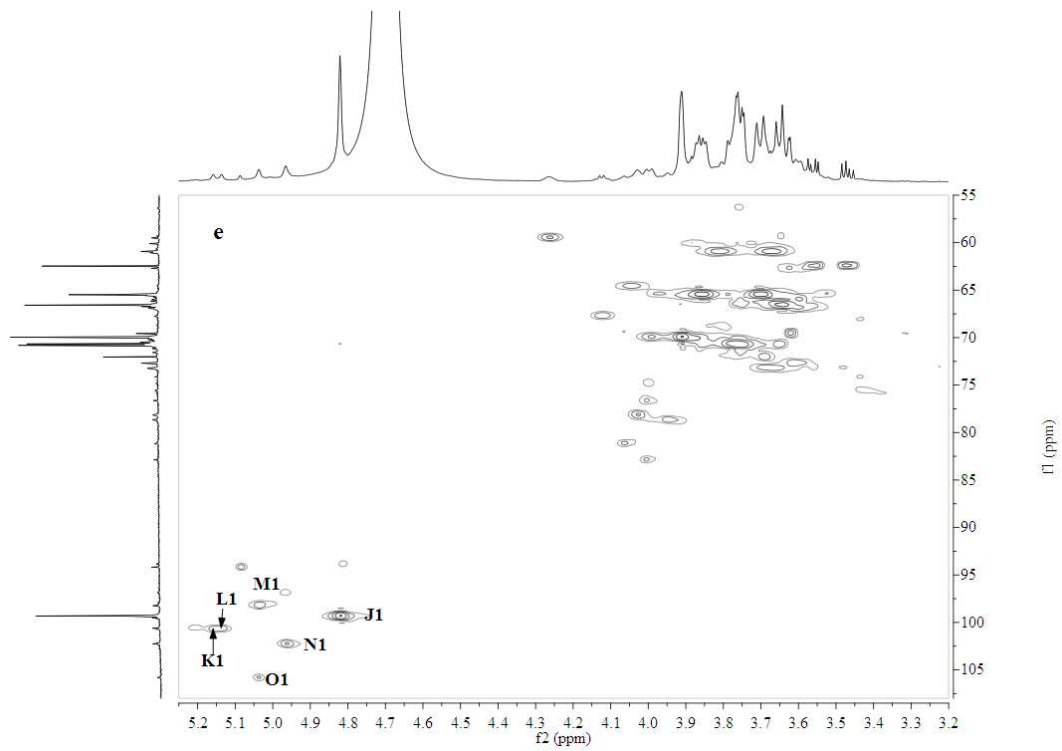

496

497

498

499

500
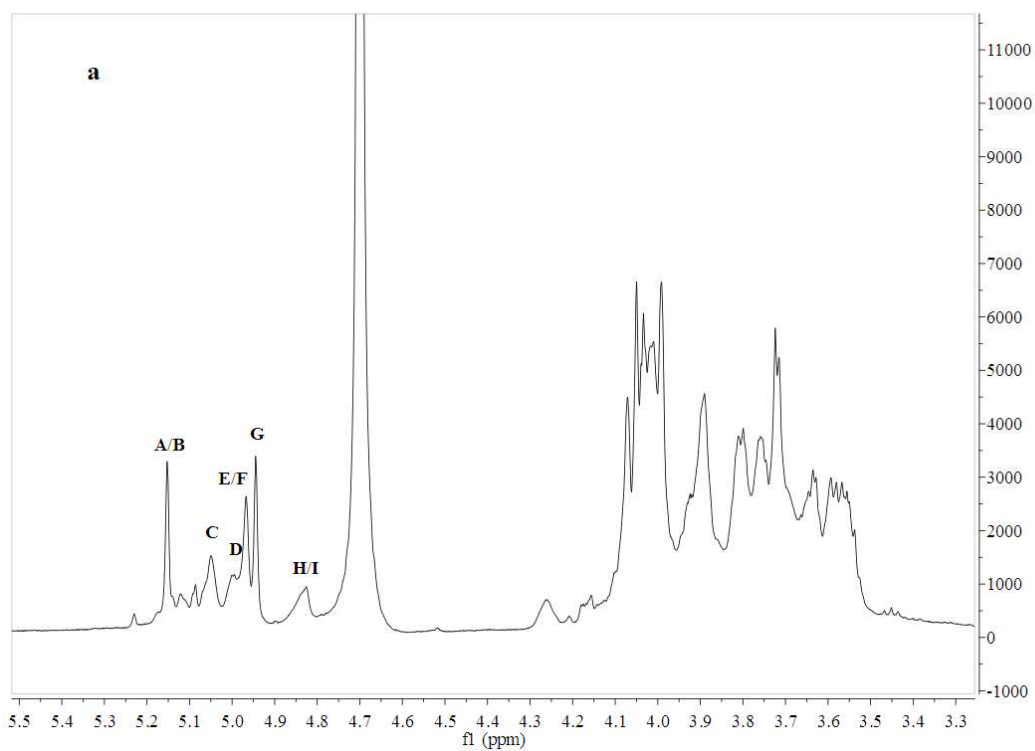
Figure 3
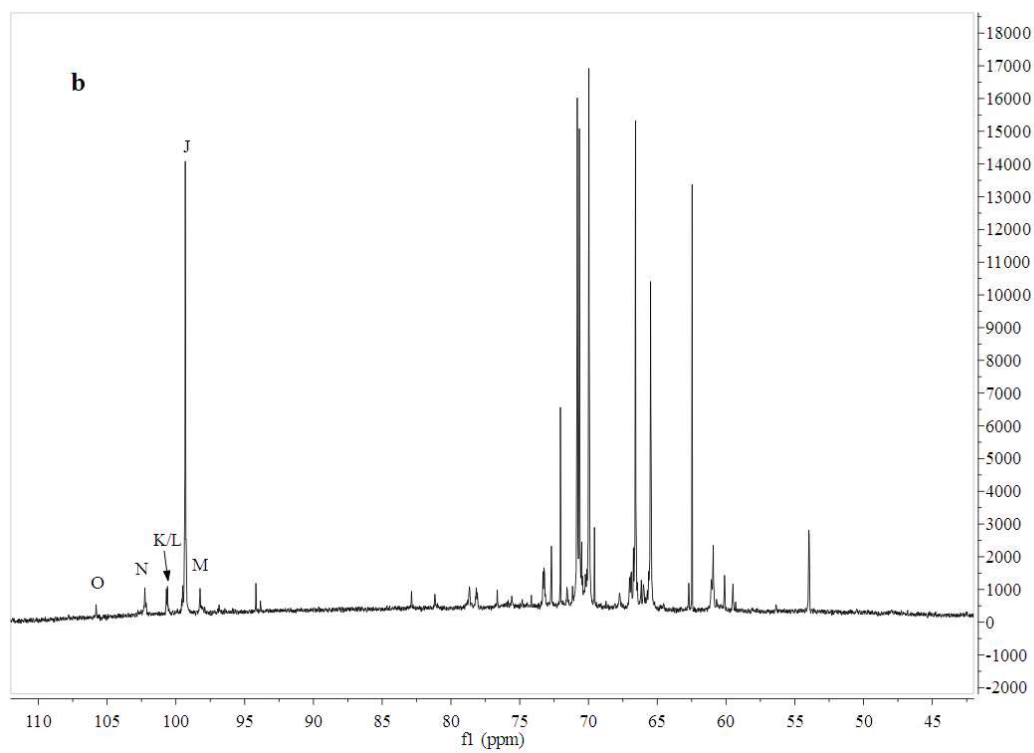
508

509

510
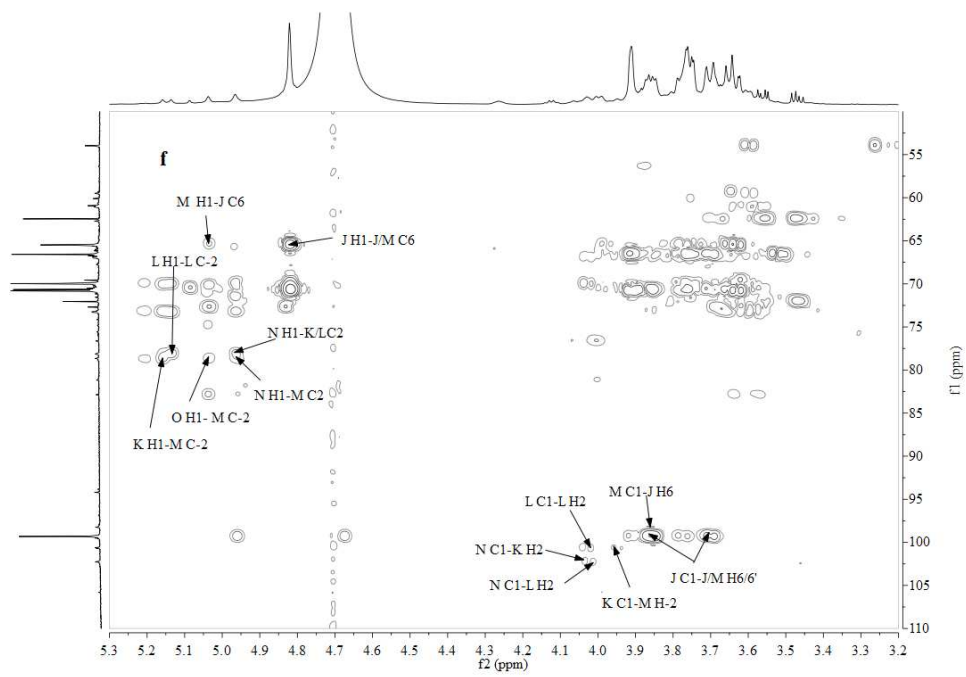
511
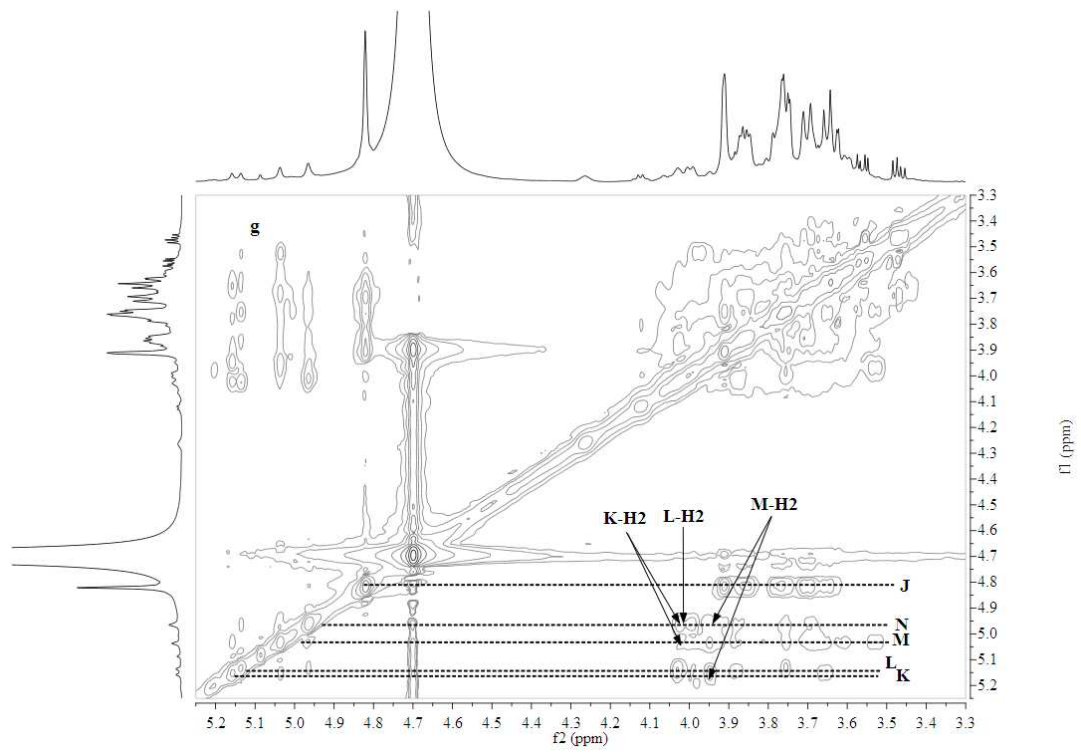
512

513

514

515

516

517 **TABLES**

518

519 **Table 1 Monosaccharide composition of the galactomannan and its hydrolysates after partial**

520 **acid hydrolysis**

Monosaccharide	galactomannan	Proportion (%)					
		Inside of dialysis bag			Outside of dialysis bag		
		0.5 h	1 h	2 h	0.5 h	1 h	2 h
Rha	0.67	1.37	nd	nd	nd	nd	nd
Gal	68.65	22.17	2.77	3.96	97.57	94.65	90.62
Glc	6.65	5.80	7.57	13.82	2.43	1.78	2.79
Man	24.02	70.66	89.66	82.22	nd	3.57	6.59

521 nd not detected.

522

523

Table 2 GC-MS of alditol acetate derivatives from the methylated products of the

galactomannan and its hydrolysate (2h-I)

Retention time	Permethylated alditol acetate	Mol (%) [a]		Deduced Linkage type
		galactomannan	hydrolysate (2h-I)	
28.44	2,3,4,6-Me$_4$ Glc and Man	5.03	15.59	T-Glc$p$/Man$p$
28.69	2,3,5,6-Me$_4$ Gal	16.72	3.33	T-Gal$f$
29.26	2,3,4,6-Me$_4$ Gal	0.78	1.88	T-Gal$p$
31.85	3,4,6-Me$_3$ Man	6.72	7.37	1,2-Man$p$
31.98	2,4,6-Me$_3$ Glc	nd	3.38	1,3-Glc$p$
32.06	2,3,6-Me$_3$ Gal	18.54	0.79	1,5-Gal$f$
32.32	2,3,6- Me$_3$ Glc	1.87	0.89	1,4-Glc$p$
32.38	2,4,6-Me$_3$ Gal	nd	0.71	1,3-Gal$p$
33.03	2,3,4-Me$_3$ Man	11.03	51.98	1,6-Man$p$
33.76	2,3,5-Me$_3$ Gal	10.55	0.36	1,6-Gal$f$
34.53	4,6-Me$_2$ Glc	1.47	0.68	1,2,3-Glc$p$
35.05	3,6-Me$_2$ Man	0.62	nd	1,2,4-Man$p$
35.81	2,3-Me$_2$ Man	4.76	2.95	1,4,6-Man$p$
36.27	3,4-Me$_2$ Man	15.56	7.25	1,2,6-Man$p$
36.73	2,4-Me$_2$ Man	1.21	2.13	1,3,6-Glc$p$
37.25	3,6-Me$_2$ Gal or Glc	0.99	nd	1,2,4-Gal$p$/Glc$p$
39.39	3-Me Man	4.17	0.70	1,2,4,6-Man$p$

526 nd: not detected.

527 [a] molar ratio of each sugar residue is based on the percentage of its peak area.

528

529

Table 3 ¹H and ¹³C NMR chemical shifts of the galactomannan (2h-I) in D_2O at 294 K.

	Residues	H1/C1	H2/C2	H3/C3	H4/C4	H5/C5	H6/C6	H6'
A	β-1,6-Gal*f*	5.15	4.08	3.99	4.00	3.90	3.81	3.56
		107.26	81.52	76.96	83.16	69.89	69.52	
B	α-1,2-Man*p*	5.15	4.04	3.90	-[a]	-	-	-
		101.24	76.96	69.87	-	-	-	
C	β-1,6-Gal*f*	5.06	4.08	3.99	4.00	3.90	3.81	3.56
		106.13	81.52	76.96	83.16	69.89	69.52	
D	α-T-Glc*p*	4.99	3.53	3.64	3.44	3.62	3.82	3.72
		98.38	71.33	72.93	72.35	73.04	61.30	
E	α-1,2,6-Man*p*	4.96	4.04	-	-	-	-	-
		97.35	76.96	-	-	-	-	
F	β-T-Gal*f*	4.96	4.05	3.99	4.00	3.75	3.64	3.59
		108.12	81.44	76.96	83.16	70.99	63.05	
G	β-1,5-Gal*f*	4.94	4.05	4.04	4.03	3.89	3.72	3.72
		108.12	81.44	76.96	83.14	75.91	61.30	
H	α-1,2,4,6-Man*p*	5.07	4.08	-	-	-	-	-
		100.84	76.61	-	-	-	-	
I	α-1,6-Man*p*	4.83	3.91	3.75	3.63	-	3.88	3.69
		99.84	69.89	70.99	66.69	-	66.34	

[a] not obtained due to low resolution.

Table 4 The ^{1}H and ^{13}C NMR chemical shifts of the hydrolysate (2h-I) in D$_2$O at 313K

	Residues	H1/C1	H2/C2	H3/C3	H4/C4	H5/C5	H6/C6	H6'
J	α-1,6-Man*p*	4.82	3.91	3.75	3.65	3.78	3.70	3.86
		99.31	69.91	70.67	66.53	70.64	65.43	
K	α-1,2-Man*p* [a]	5.16	4.03	3.88	3.69	3.81	3.67	3.81
		100.67	78.09	70.09	70.69	-[c]	60.9	
L	α-1,2-Man*p* [b]	5.14	4.02	3.87	3.66	3.79	3.67	3.81
		100.61	78.09	70.09	70.69	-	60.9	
M	α-1,2,6-Man*p*	5.03	3.95	3.89	3.61	-	3.70	3.86
		98.16	78.63	70.14	69.50	-	65.43	
N	α-T-Man*p*	4.96	3.99	3.76	3.57	3.68	3.68	3.80
		102.22	69.91	70.67	66.91	73.14	60.91	
O	β-T-Gal*f*	5.04	4.06	4.00	4.01	-	-	-
		105.78	81.07	76.62	82.84	-	-	

535   [a] the residue was linked with →2,6)- α-D-Manp-(1→

536   [b] the residue was linked with →2)- α-D-Manp-(1→

537   [c] not obtained due to low resolution.

538